Enabling the Decarbonization of Regional Air Transport with Series Hybrid Electric Propulsion

Dimitrios Bermperis¹, Stavros Vouros², and Konstantinos Kyprianidis¹

¹Future Energy Centre, Mälardalen University, Västerås, Sweden
E-mail:, dimitrios.bermperis@mdu.se, konstantinos.kyprianidis@mdu.se

²School of Innovation, Design, and Engineering, Mälardalen University, Västerås, Sweden
E-mail:, stavros.youros@mdu.se

Abstract

The aviation industry faces significant environmental challenges, prompting the implementation of regulations to mitigate the adverse effect of carbon-based energy and associated emissions. While electrified flight is a promising pathway, limitations in battery specific energy narrow down the application space to commuter and regional classes. Towards that direction, this work investigates the design and operation of a series hybrid electric 30-passenger regional aircraft. A multi-disciplinary framework is utilized, comprising modelling approaches for multi-point engine design, physics-based electrical component sizing and performance, aircraft sizing, mission design, and environmental assessment. Electrification facilitates novel propulsion architectures that enable the installation of propulsors in unconventional locations. In that regard, distributed propulsion with up to three propellers per wing is evaluated for aerodynamic benefits. With optimal wing redesign, drag reduction benefits reach 4% for the selected aircraft class. Variable free power turbine speed operation and one engine-off during descent are promising synergetic concepts, delivering further electrification gains. A combination of hybridization during take-off, climb and cruise defines the optimal design and operation guidelines for the hybrid concept. The trade-off between applying the electrification strategy and having an integrated engine and aircraft design, matching all top-level aircraft requirements is highlighted. Excessive battery mass confines the favorable design space, revealing a threshold in the range of 1-1.2 kWh/kg for series hybrid electric aircraft that outperform same Entry-Into-Service conventional configurations.

Keywords: series hybrid electric, regional flight, conceptual design, distributed propulsion

1 Introduction

The aviation industry is assessing several technologies in order to decarbonize the sector. Among those, electrification holds potential for regional flight. Several hybrid electric concepts have been investigated in the literature with varying degrees of fidelity in the underlying models [1–3]. This work focuses on the series hybrid electric concept, which despite its system complexity could lead to environmental and consumption benefits through several synergetic opportunities.

Different parallel and series hybrid electric concepts were compared for several Entry into Service (EIS) years by Nasoulis et al. [4]. Compared to a conventional configuration with EIS 2014, the 19-passenger series hybrid electric concept overperformed the parallel one with greater block

fuel reduction for the same evaluated mission of 400 NMI. The authors showed that the series aircraft is more efficient in terms of life cycle costs as well. Environmental benefits in the order of 60% were noted, for assumed battery cell characteristics of 0.7 kWh/kg, paired with gas turbine performance improvements in the order of 20% between the investigated EIS configurations. On the other hand, Dean et al. concluded on the opposite outcome when comparing the series and parallel configurations [5]. For same battery technology and simulated mission, they found that the parallel hybrid concept offers better performance. Ludowicy et al. investigated light aircraft with the series propulsion architecture and multiple propellers per wing for distributed propulsion benefits [6]. They highlighted that an optimized distributed propulsion concept can prove to be competitive with today's

conventionally powered light aircraft, while enabling significant fuel savings. Finally, the series configuration was investigated by Schroeter et al. for regional aviation with a 70-passenger aircraft on a mission of 400 NMI [7]. They found that the optimal degree of hybridization (DoH) lies in the range of 30-40% for their specific assumptions. Those levels of electrification led to block energy reduction, while higher ones offered reduced advantages at higher mission lengths.

Distributed propulsion (DP) was investigated at the preliminary design level by de Vries et al [8]. They produced an analytical method to estimate the aerodynamic benefits. They highlighted that DP improves lift to drag ratio at cruise by 6%, however, energy consumption increases around 3% due to added mass. In a similar study, using medium fidelity aeropropulsive simulation, Ma et al. noted that 8 propellers showcased the best results with a 11% benefit in lift-to-drag ratio and 6% increased mission range due to reduced drag [9]. Borer et al. investigated distributed propulsion designs for the NASA X-57, noting that competitive cruise performance is achievable [10]. Finally, a 3% reduction in aircraft power requirements is reported by Keller in DP concepts, driven by wing tip propellers installation and wing redesign [11].

There is a wide range of claimed environmental performance benefits for the series hybrid electric concept, which is driven by discrepancies in performance assumptions, modelling simplifications, and the large number of potential synergetic concepts. In an effort to provide consistent and comparable outcomes, this work utilizes a thoroughly verified integrated conceptual design approach and framework for the series hybrid case, which has also been used for assessing all other hybrid electric variants [1], offering a platform for fair comparisons. At the same time, the interactions and driving design and operation principles of different onboard power system are tied to the mission-level performance, revealing the potential and bottlenecks of series electrification. Through this structured process of conceptual design, the technology thresholds for competitive series regional flight are identified.

2 Methodology

A 30-passenger aircraft, representative of regional and commuter flight, is used as the starting vessel for this investigation. The reference conventional Jet-A aircraft carries two wing mounted turboprop engines. This aircraft is derived according to [1] and is based on Dornier 328-100. A turboelectric variant with two aft mounted turboshaft engines coupled to generators, and one electrically driven propeller per wing is designed. Wing loading is kept constant between the turboelectric and conventional EIS 2035 variants. The two-propeller turboelectric configuration acts as the hybrid electric case of reference for following relativized outcomes. A battery system is added for series hybrid electric concepts. Both series and turboelectric variants facilitate variable Free Power Turbine (FPT) speed operation and Distributed Propulsion due to the decoupling of gas turbine and propeller shafts and the possible installation of multiple propellers per wing. Such a series configuration is depicted in **Figure 1**. Both synergetic concepts are evaluated in the respective Results Sec-

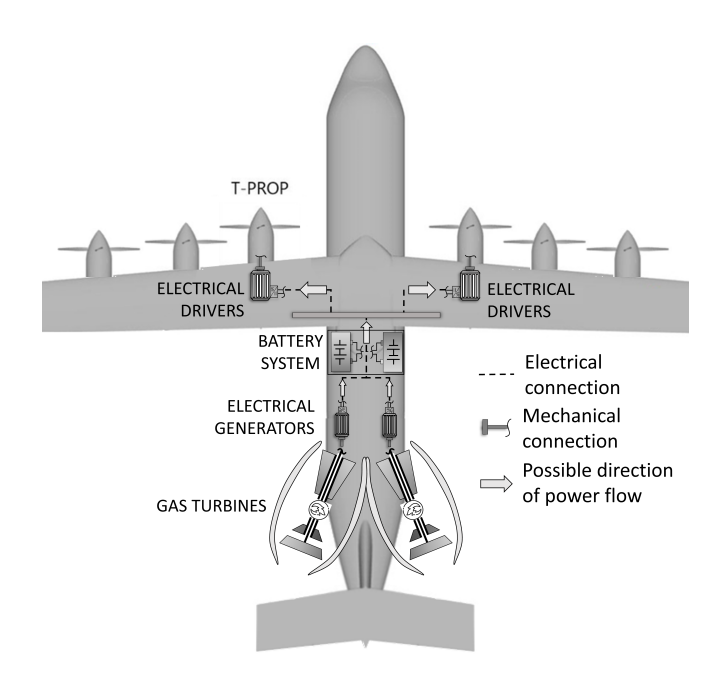


Figure 1: Series hybrid electric configuration with distributed propulsion

tions. All hybrid electric technologies are assumed to have an Entry-Into-Service year of 2035. Design mission is 1000 NMI, diversion 250 NMI, and loiter scheduled for 30 minutes. Cruise altitude is 20 kft at 0.53 Mach. Reference conventional and turboelectric aircraft assumptions and boundary conditions are given in **Table 1**.

2.1 Turboshaft and Propeller

An engine model is developed to design and evaluate the performance of the gas turbine powerplant for all evaluated concepts and configurations herein. The model is built within the aeroengine conceptual design tool EVA [12] and integrated within a multidisciplinary design framework discussed in [1]. The turboshaft engine is a 2.5-spool geared turboprop configuration with an all-axial seven-stage gas generator compressor (GGC), an axial cooled two-stage gas generator turbine (GGT) and an axial uncooled three-stage free power turbine, which is coupled to a generator and the respective electrical branch components. A single speed propeller coupled to an electric motor and the respective electrical branch components completes the gas turbine and propulsor system.

A multipoint synthesis approach and design point matching scheme have been applied for all engines. Metal temperatures at take-off for the two-stage GGT are set to 1170K, based on the material maturity assumptions [13]. A parametric cycle design study was carried out to determine cruise Overall Pressure Ratio (OPR) and Turbine Rotor Inlet Temperature (T41) at 12.5 and 1250K, respectively. This choice ensured acceptable GGC last stage blade height, and favorable cruise specific fuel consumption as well as turboshaft and propeller dry weight. Propeller diameter and rotational speed are decided for cruise propeller loading of 100 kW/m² and cruise propeller tip speed of 220 m/s, according to Kavvalos et al. [14]. The multipoint matching scheme ensures that all targets are

Table 1: Assumptions and boundary conditions for reference aircraft

Specifications	Dornier	EIS 2035	EIS 2035 Turboelectric			
GENERAL	328-100	Convent.				
Passengers, [-]	30-32	30	30			
Payload, [kg]	3150	3150	3150			
Range, [nmi]	1000	1000	1000			
CR altitude, [kft]	20-25	20	20			
CR speed, [Ma]	0.53	0.53	0.53			
WING						
Area, [m ²]	40	30.8	38.3			
Aspect ratio, [-]	11	11	11			
Wing loading, [kg/m ²]	350	400	400			
PERFORMANCE						
$MTOW, \Delta(\%)$	Ref.	-11.8	+9.5			
Block fuel, $\Delta(\%)$	Ref	-12.3	-0.1			
TOP-LEVEL AIRCRAFT REQUIREMENTS						
Take-off field length, [m]	Ref.	1350	-			
Rate of climb, [ft/min]	Ref.	1725	-			
Approach speed, [m/s]	Ref.	52.5	-			

achieved, and only feasible powertrain designs are generated. A detailed discussion of the scheme and cycle parameters selection is provided in [14–16]. Cycle design and metal temperatures are constant throughout the evaluation.

2.2 Electrical Power System

The electrical component models and a dedicated investigation of trade-offs and synergies at play have been shown by Bermperis et al. [17]. Simulated electric machines are of the permanent magnet synchronous topology for their advantage in terms of specific power. Analytical and physics based 1D models are developed and utilized. An equivalent thermal resistance model with multiple nodes is used to calculate and monitor operational temperatures. For power electronic converter components, a lumped thermal model is combined with sizing equations fitted to publicly available data for state-ofthe-art components and scaled for the projected EIS year. Performance of power electronic components is estimated in a time-average manner capturing conduction and switching losses. DC cables are sized according to ambient conditions and altitude of operation, taking into consideration the lower air density. The sizing and performance model of the battery refers to Li-ion cells. Cell characteristics are scaled to packlevel accounting for auxiliary components and connections. Heat exchange surfaces are designed for safe battery operation. A resistance-capacitance equivalent model is combined with a scaled Shepherd's model for battery system performance [18], capturing charging and discharging.

The integrated electrical power system comprises of three branches. A battery system and DC bus bar span the fuselage and connect all electrical branches together, acting as the power management and distribution node. The branch coupled to the propellers comprises an axial-flux permanent magnet synchronous motor, cooled via an external finned jacket. The electric motor is coupled with a SiC DC/AC inverter for control. The electrical branch coupled to the turboshaft comprises a radial-flux permanent magnet synchronous generator. An external jacket is used for this machine as well, with liquid cooling. A SiC AC/DC rectifier controls the generator. A DC/DC converter connects the branch and DC bus bar. For all branches, power is transmitted through aluminium DC power cables.weight, and therefore variation of thrust requirement.

2.3 Mission and Aircraft Analysis

Aircraft design and mission calculations are made withing the EVA tool [12]. A predefined key aircraft geometry is used for dimension modelling of any new aircraft configuration based on the rubberized wing methodology [19]. Sizing and analysis of each airframe component is performed to reach an aircraft weight estimation [19-21]. Aircraft aerodynamics are modelled according to principles described by Jenkinson et al [19]. Aircraft drag polar is predicted during the mission for individual components based on aircraft geometry and high lift device settings [19-21]. Aircraft performance modelling is based on methods described by Jenkinson et al. [19] and Roskam [20]. Calculations include a main and diversion mission. All following results refer to main mission outcomes, however, inclusion of reserves and diversion mission in the design loop is fundamental as it impacts aircraft weight and aerodynamics. Cruise performance is calculated in a discretized manner to account for on-flight fuel consumption, gradual reduction of carried weight, and therefore variation of thrust requirement.

 ${\rm CO_2}$ and ${\rm NO_x}$ emissions complete the integrated framework. ${\rm CO_2}$ gaseous emissions are directly related to fuel burnt. Complete combustion is assumed. ${\rm NO_x}$ emissions are calculated with a semi-empirical expression, derived for modern rich-burn quick-quench lean-burn single-annular combustors [12, 22]. The correlation is based on simulated data and corresponding ${\rm NO_x}$ emissions measurements from the ICAO engine emissions databank. Noise production is also crucial for regional aircraft. Detailed noise generation and propagation modelling is out of scope in this work, however, for isolated propeller effects, a constant and acceptable propeller tip Mach number is prescribed. Moreover, several community efforts support hybrid electric and distributed propulsion design for noise regulation [23–25].

2.4 Series Hybrid Operation and Distributed Propulsion

In the series hybrid configuration, all propulsors are driven by electrical machines. Power is provided by turboshaft engines and battery systems. Mechanical power is converted to electrical with generators. Hence, power reaching the propulsors comes from the battery, accounting for transmission losses and the turboshaft, accounting for conversion losses. If battery energy is not expended, the configuration operates in turboelectric mode, where all power required by the propulsors

is provided by turboshafts and fuel, taking into consideration losses of intermediate electrical components.

Since all propulsors can be electrically driven, multiple ones may be installed across the wing. This is not an effective option in the conventional case, due to the associated losses and complexity of installing multiple smaller turboprop engines in the wing. The distributed propulsion concept aims to take advantage of local flow acceleration across the wing to enhance aircraft aerodynamic performance. Increased effective speed across a wing of given area, facilitates the generation of the same lift force with a lower lift coefficient, or can allow for greater lift generation under unchanged angle of attack. Increased effective speed also impacts wing drag, which will increase if no wing redesign takes place. Hence, there is a trade-off in the aircraft aerodynamics dictated by the propeller jet velocity and the coverage of propulsors across the wing. To calculate the effective wing velocity due to distributed propulsion, the following equation is used to estimate the wingspan fraction covered by the propeller jet velocity [8]. The later is calculated via actuator disk theory. To estimate the new average wing effective speed, ΔY acts as the weight of the propeller jet velocity and $(1-\Delta Y)$ acts as the weight of the flight speed.

$$\Delta Y = \frac{N_p \cdot D_p}{\left(b/2 - D_f/2\right)} \tag{1}$$

 ΔY is the wing coverage percentage, N_p the number of propellers per wing, D_p the propeller diameter (assumed equal for all), b the wingspan, and D_f the fuselage diameter.

3 Results

3.1 Novel Synergies via Series Hybridization

3.1.1 Design with Distributed Propulsion

Three distributed propulsion cases are evaluated for potential drag reduction benefits. One propeller per wing does not constitute a DP concept, but it is still evaluated with the same aerodynamic rules and equations. Nonetheless, the one propeller case, with no aeropropulsive interactions accounted for, is reported ("*1-ref.*") and acts as the reference for **Table 2**. Under constant propeller tip speed velocity and cruise loading, propeller diameter reduces for increasing number of propellers. Design speed follows the inverse trend. Wing coverage for the derivation of wing effective speed increases, with a reduced rate for more installed propellers. EPS losses increase, as the propeller driving motor branch is designed with smaller and slightly less efficient components.

Distributed propulsion facilitates the increase of wing loading via wing area reduction, because the same lift is generated more effectively. Benefits in aerodynamic performance come from this wing redesign [8]. The critical wing loading design point occurs at landing conditions. Hence, the approach speed is set as a top-level aircraft requirement (TLAR), while the propellers per wing increase. As shown in **Table 2**, simply accounting for the aeropropulsive interactions, allows for an 11.5% wing loading increase, while reaching up to three propellers leads to 20.6%. The effect of wing aeropropulsive

Table 2: Key propeller design parameters in distributed propulsion

Propellers per wing	Units	1	2	3
Diameter	$\Delta[\%]$	-1.3	-30.7	-43.5
Design Speed	$\Delta[\%]$	+1.3	+44.2	+77.0
Wing Coverage	[%]	30.6	44.3	55.2
Wing Loading	$\Delta [\%]$	+11.5	+16.7	+20.6
EPS losses	[%]	14.2	15.0	15.2

interactions in take-off conditions is also captured by an increase in CL_{max} , according to the combined methodologies of [8, 26, 27]. That change, along with the effect of the increased wing effective speed, yield the reduction of wing area.

Key propulsion parameters are captured in Figure 2. Power required by the propulsors is reduced up to 4.5% and it correlates directly with the reduction of required thrust, which is driven by the reduction of drag due to improved aerodynamic performance. Drag reduction is a combined effect, dictated by the reduction of wing area and thus mass contribution to the total aircraft weight, reduced friction drag in wings due to size, the snowball effect of reducing fuel and therefore carried mass, and the improved lift over drag. Aspect ratio is kept constant during wing redesign. Block fuel does not reduce with the same rate as the required aircraft power. This is a direct outcome of the deteriorating conversion efficiency of the intermediate electrical components, that comes with the increasing number of propulsors. Hence, power generated by the turboshafts, which dictates fuel consumption, reaches a -3.25% change for the configuration with three propellers compared to the conventional reference.

It is noted, that roughly half the amount of any reported benefit comes from simply accounting for the aeropropulsive interactions, while the rest comes from the impact of increasing

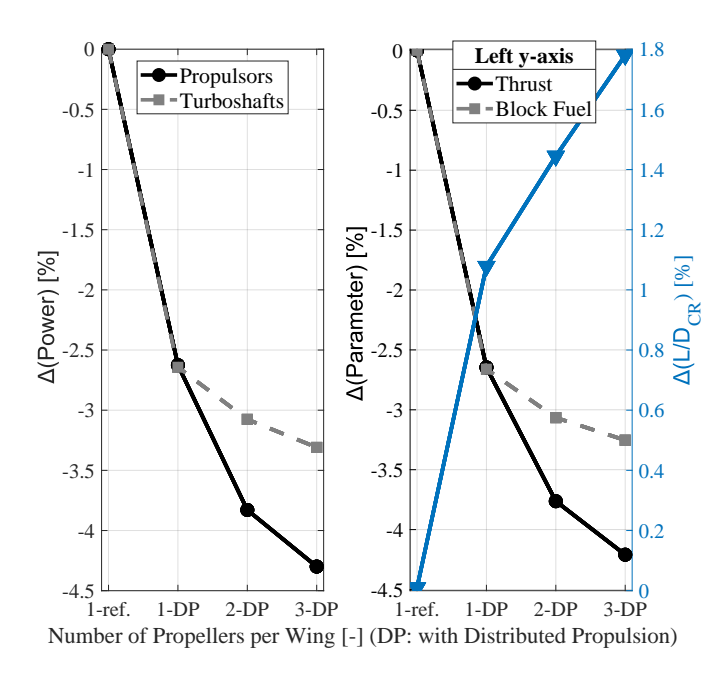


Figure 2: Variation of power requirements and performance for different distributed propulsion configurations with turboelectric propulsion architecture

the propulsors per wing. Greater benefits could be achieved, for propellers of lower original power loading, hence, larger diameter and more wing coverage.

3.1.2 Free Power Turbine Speed Selection

The series hybrid electric propulsion architecture enables full decoupling between propeller propulsors and the free power turbines, which usually drive them in conventional configurations via direct shaft coupling and gearboxes. The turboshaft engines are coupled with electrical generators, and the propellers with electrical motors. Through power controllers that drive the electrical machines, operating speeds can be regulated. Hence, the propulsion system designer may choose the free power turbine speed that leads to best system performance for each phase of the mission.

Performance and sizing variations in turboshaft engines, propellers and the electrical branch that is coupled to the turboshaft are presented in Figure 3. Free power turbine speed directly correlates to the coupled generator speed, since they are connected with a fixed ratio gearbox. Therefore, this speed choice should yield optimal performance for the turbomachinery and electrical components. Given that sizing of electrical components is based on whole mission profile requirements, and the turboshaft and propellers are designed with a multipoint synthesis scheme, the selection of FPT operational speeds leads to both sizing and performance changes. Each column of Figure 3 corresponds to the respective investigated mission phase. FPT speed is varied relative to Top of Climb design speed which is kept constant throughout this study. Speed variation for each segment differs and is constrained by turbine operational limitations due to overspeeding or insufficient speed for the required thrust and pressure ratio design. The design space is also such that the turbine loading justifies the selection of three turbine stages, and the disk stresses are always sufficiently bellow critical limits.

Variations in turboshaft performance are directly correlated to the position of the operating point in the turbine map with respect to the efficiency islands. It is observed that a certain overspeed percentage is advantageous in all cases but descent. This indicates that those points lie to the left of the optimal performance island in the map. The opposite is true for descent. The specific fuel consumption depicted is the uninstalled one. Nevertheless, installed SFC coincides almost 100% with the former, given that mass changes are relatively small due to the FPT being only a part of the engine. Given that the design point speed is kept constant in this investigation, only the variation of cruise FPT speed affects sizing, and results in mass changes. Variation of cruise efficiency affects cruise performance and the pressure ratio to achieve a prescribed power requirement. Therefore, the mass variation trendline follows the SFC line of that segment, which is the invert of turbomachinery efficiency. Worse efficiency correlates to larger component areas, and larger turboshaft mass. Two performance plots are included for descent. In the bottom, another novel operational concept facilitated by series hybridization is examined. The detailed investigation is given in **Section 3.1.3**. When one engine is off during descent, the one that still operates experiences almost double the loading. This moves the operational point in the map and affects the speed variation impact on propulsion system performance.

Electrical power system mass for the branch coupled to the turboshaft engine is closely related to prescribed speed vari-

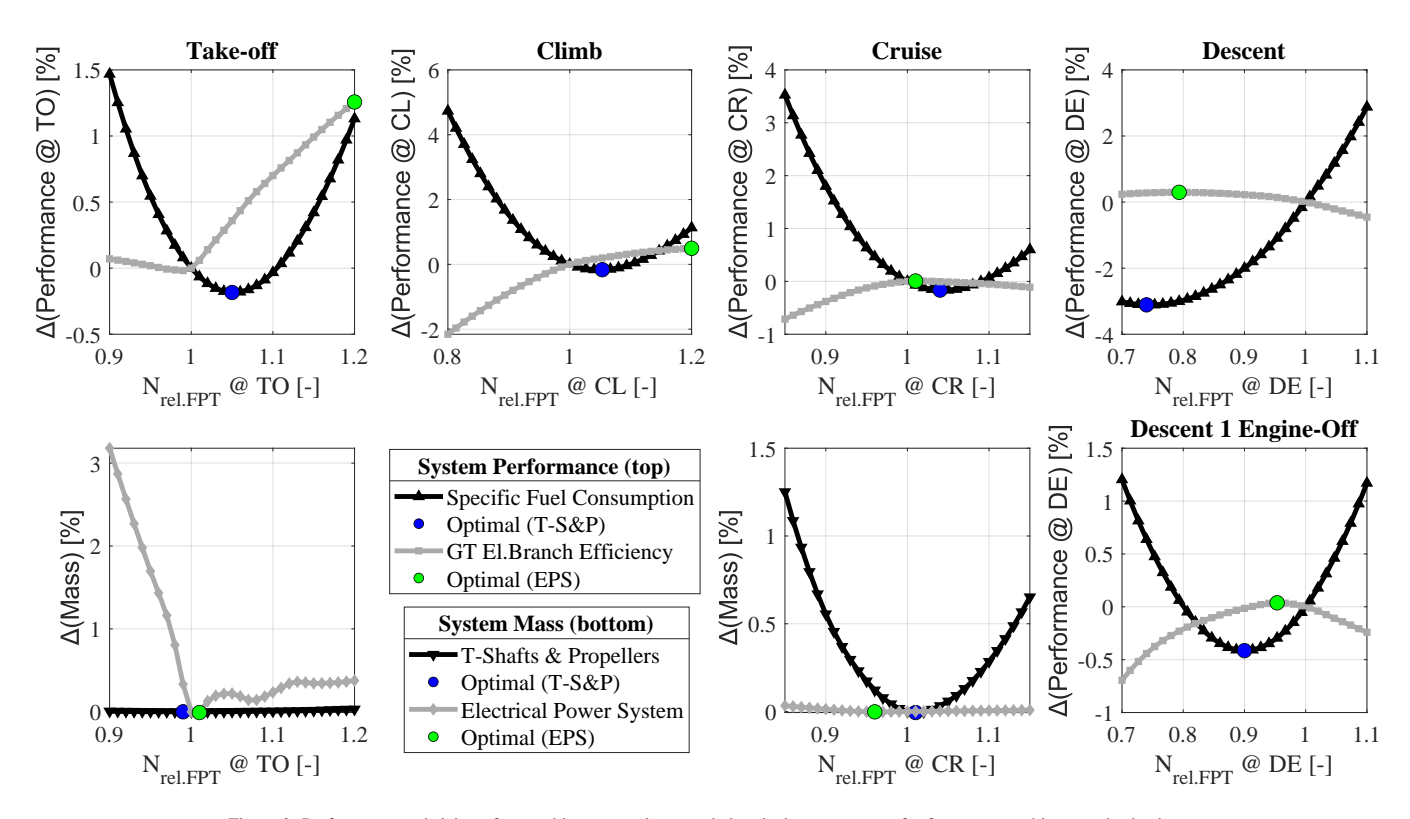


Figure 3: Performance and sizing of gas turbines, propulsors, and electrical power system for free power turbine speed selection

ations. This is apparent only in changes made to take-off conditions. Generator power is greatest during take-off, which for the reference case of constant FPT speed across the envelop, translates to peak torque requirements. Therefore, the branch sizing point is at take-off. When FPT speed at take-off is reduced for constant power output, the generator torque input increases, which raises design point torque requirement. This leads to a sharp mass increase, leftwards of the reference point. On the other side, when FPT and generator speed at take-off are increased, the torque input at take-off conditions is reduced. Peak torque requirement for the generator is not at take-off conditions anymore, as other points are operated at lower speeds with similar power requirements, therefore greater torque. Hence, the generator mass is no longer varied for take-off FPT speeds above the reference value. Nevertheless, rest of the electrical branch components are resized as a function of the maximum voltage and current found across the envelop, and varying losses which change the design conditions of subsequent components. As take-off speed increases, the voltage produced by the generator increases as well. This leads to an increase of power electronic modules needed. Increased voltage has a positive effect on cable mass. The outcome is a relatively smaller increase of mass for overspeed conditions, due to the outcome of those competing factors.

With respect to performance, variation of speed at constant design conditions leads to a movement of the operational points around the efficiency islands of the performance map, similarly to turbomachinery components. Efficiency is a function of power and speed loading. The electric generator drives branch performance trends, and the final outcome is affected by the original placement of reference points.

Selecting the FPT operating speed, and consequently affecting sizing and performance of the electrical branch and turboshaft engine is a complex matter. Cruise is the longest segment, and the designer aims to optimize performance there. When a compromise between EPS and turboshaft performance needs to be made, one has to consider multiple effects. Worse SFC leads to more fuel carried on board. On the other side, worse electrical system performance results in greater power output needed from the FPT to power the propulsors in turboelectric mode, or less efficiently utilized electrical energy which increases fuel dependency. Optimal speed selection needs to be made at the aircraft level and with respect to overall aircraft performance. However, the underlying propulsion system trends are necessary to be acknowledged in order for the speed selection to be justified.

3.1.3 Descent One Engine-Off

During descent, low thrust is required to achieve the prescribed trajectory. Hence, the turboshaft engines are pushed to low power loading. This leads to degraded fuel performance during the segment. Decoupling the propellers and turboshafts via the intermediate electrical power branches allows for one of the two turboshafts and corresponding generator-driven electrical branch to be disengaged and turned off during descent. Thus, all descent power comes from and passes through one turboshaft and connected electrical branch (all motor-driven branches and propellers operate), raising the relative load and pushing operation in theoretically better performing regions. The analysis is presented in **Figure 4**.

Reference case is the fully turboelectric configuration with two operative engines at descent. The test case examined, for both one engine-off and regular two engines-on concepts, is the 10% ascend hybridization with 5% cruise hybridization. Drawing all aircraft required power from one engine, would presumably lead to double power output from the one operative. However, electrical branch efficiency improves by roughly 1%, which results in less transmission losses. Thus, for certain thrust and power propeller requirement, less descent power is needed when only one turboshaft engine operates, compared to two. This leads to an 89% increase in one engine's power between the two concepts. Increasing the relative loading in such a way, moves the descent operating point closer to the design and cruise points, which have the nearoptimal performance. This is indicated by the 22% reduction in SFC, 1% increase in electrical efficiency and, finally, 30% decrease in descent required fuel. These benefits yield a 3.5% drop in block fuel which is an 1.5% improvement from the two engines-on during descent concept for the same degrees of hybridization. It is noted that when the hybrid electric aircraft is operated in shorter missions than the design one, the impact of descent fuel reduction on block fuel will be more pronounced due to the relative change in segment durations.

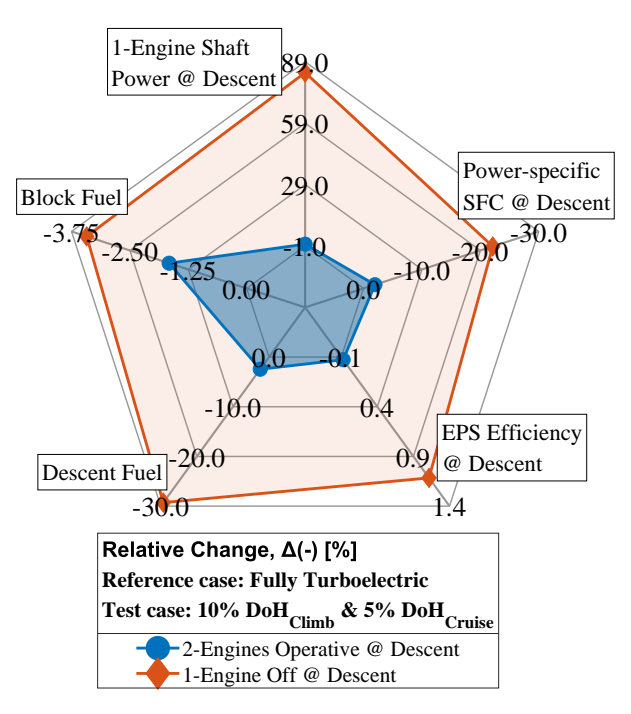


Figure 4: Impact of one engine-off operation during descent

3.2 Series Hybridization Design and Operation

3.2.1 Hybridization Schemes and Propulsion Design

Bringing electrical energy on board in the form of batteries comes with mass penalties. Propulsion system and aircraft redesign to match the original aircraft's top-level re-

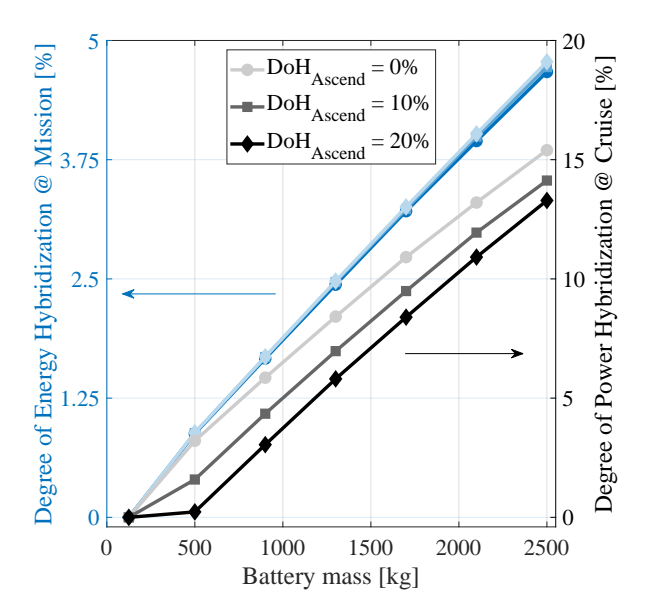


Figure 5: Change of degree of hybridization with battery mass for different ascend hybridization levels

quirements are necessary. The former is usually upsized to provide greater thrust for a heavier aircraft and the latter is designed with larger wings which facilitate equivalent take-off and landing performance. However, applying a hybridization scheme and tackling aircraft and propulsion system redesign simultaneously, produces complex results with underlying system dependencies.

To distinguish those effects, the impact of hybridization through sole propulsion system design is initially evaluated. Results are extended to the mission and aircraft level, but with no aircraft design changes and fixed geometries. The propulsion system is redesigned to ensure fixed climb and descent times in all cases. Power selection corresponds to across-the-envelop requirements, ensuring consistent and fair outcomes in terms of mission durations and ratings. At this section, no propulsion and aircraft redesign take place to match the original top-level aircraft requirements of take-off field length, rate of climb and approach speed. Degree of power hybrid-

ization (DoH_{power}) is defined as the power generated by the battery system, over the power produced by all power sources (battery and turboshaft).

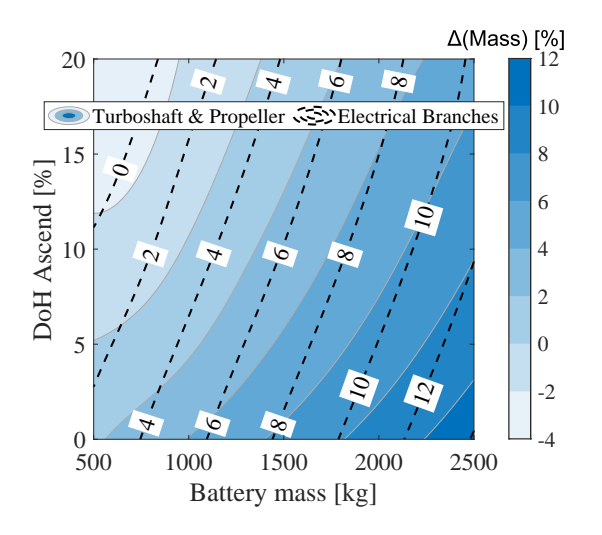
The variation of power hybridization in ascending and cruise phases is evaluated. The former is the most power demanding, and off-loading the turboshaft engine leads to better performance. The latter is the longest mission phase, and hybridization there holds great potential. Previous investigations in other hybrid concepts indicated that a combination of ascend and cruise electrification yields best aircraft performance [1]. This claim is now assessed for the series configuration.

Applied degrees of hybridization are shown in **Figure 5**. Three levels of ascend hybridization are prescribed at 0%, 10% and 20%. These values correspond to the same degree of power hybridization at take-off and climb. Battery mass is varied under constant assumed cell characteristics. Cruise degree of hybridization is calculated by the integrated framework, for 20% end of mission battery state-of-charge. All other main mission segments (descent, landing and taxi) are operated in turboelectric mode with no battery depletion. Diversion mission is operated under one energy source, therefore in turboelectric mode with complete fuel dependency.

The 0% hybridization and 125 kg of battery point corresponds to a fully turboelectric configuration, where the battery is only used to balance minor load variations. This turboelectric configuration (Table 1) acts as the reference case and all relative results are normalized against it.

Resulting degrees of power and energy hybridization at cruise are shown in **Figure 5**. Greater ascend hybridization for given installed electrical energy, leaves less available for cruise. A 15% cruise power hybridization results to about 5% energy hybridization across mission. Electrical branch efficiency is 85-90%, while gas turbine is 25-30%. Hence, for the same delivered power under a certain amount of time, more energy is required by the gas turbines. Thus, the difference in power and energy degrees of hybridization.

The variation of propulsion system and aircraft mass are depicted in **Figure 6**. Electrical power branches do not include



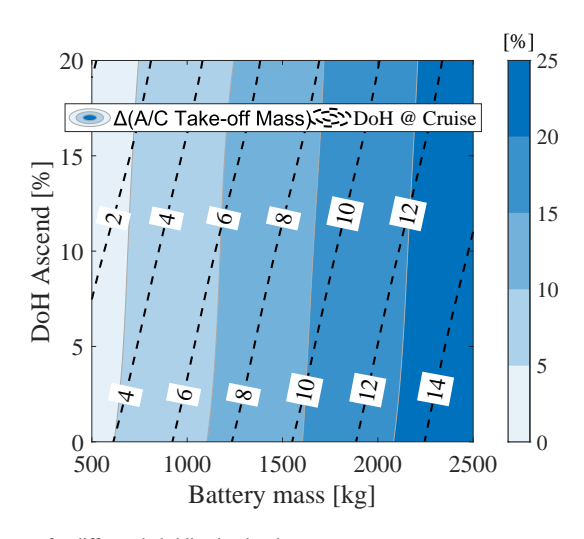


Figure 6: Propulsion system and aircraft mass for different hybridization levels

the battery, which is a design variable. Larger cruise degrees of hybridization correspond to heavier aircraft, as shown in the right diagram.

A heavier aircraft requires a propulsion system of greater thrust capabilities; hence the propellers will be upsized. Same goes for the motor electrical branches that drive them. This leads to an increase in propeller and electrical branch mass for increasing cruise hybridization. Turboshaft engine design point is at top of climb. For constant ascend electrification, turboshaft design point power follows the propulsor trend, which increases due to the increased thrust requirement of the heavier aircraft. The generator electrical branches are size in turboelectric diversion, which also scale with battery mass and increasing power requirements. For increasing ascend hybridization, aircraft mass reduces slightly for a given battery. This corresponds to a size reduction for all propulsion systems. Turboshafts become especially lighter, given that more battery dependency is scheduled at top of climb, therefore, their design conditions relax. The lightest propulsion systems are designed for high ascend and low cruise power hybridization, which does not increase thrust and reduces turboshaft design point requirements.

Block fuel is investigated to identify optimal power management directions, when propulsion design is not constrained by top-level aircraft requirements. To be able to justify resulting trends, specific fuel consumption and thrust requirement are studied, simultaneously. For the investigated ascend degrees of hybridization and battery system masses, the left column of

plots in **Figure 7** shows thrust requirement and SFC variation for climb and cruise. In cruise conditions thrust and drag are equal. Specific fuel consumption is shown as the inverse of itself. This allows to visually identify the battery mass and cruise hybridization where specific fuel consumption reduces due to hybridization relatively more than thrust requirement increases (dashed line is above continuous line).

In all examined ascend hybridization cases, cruise SFC is benefiting more from electrification, than cruise thrust requirement worsens. This overall thrust requirement increase is not matched by a respective climb SFC improvement, unless when ascend is also electrified above a certain threshold. For 0% ascend hybridization, climb fuel performance only deteriorates. At 10%, only designs with less than 1500 kg of battery mass have advantageous climb fuel performance, and at 20% the whole design space performs better during climb compared to the reference case. This effect drives greater block fuel benefits at higher ascend phase electrification.

For increasing battery mass and cruise hybridization, block fuel improves up to a certain degree - then the slope reverses. This optimal cruise hybridization point shifts to more installed battery mass for greater degrees of ascend hybridization. The adverse block fuel slope is related to the sharp rise of climb and cruise thrust requirements for increasing installed electrical power system and aircraft mass, which reach critical values and trigger a snowball effect above a certain threshold.

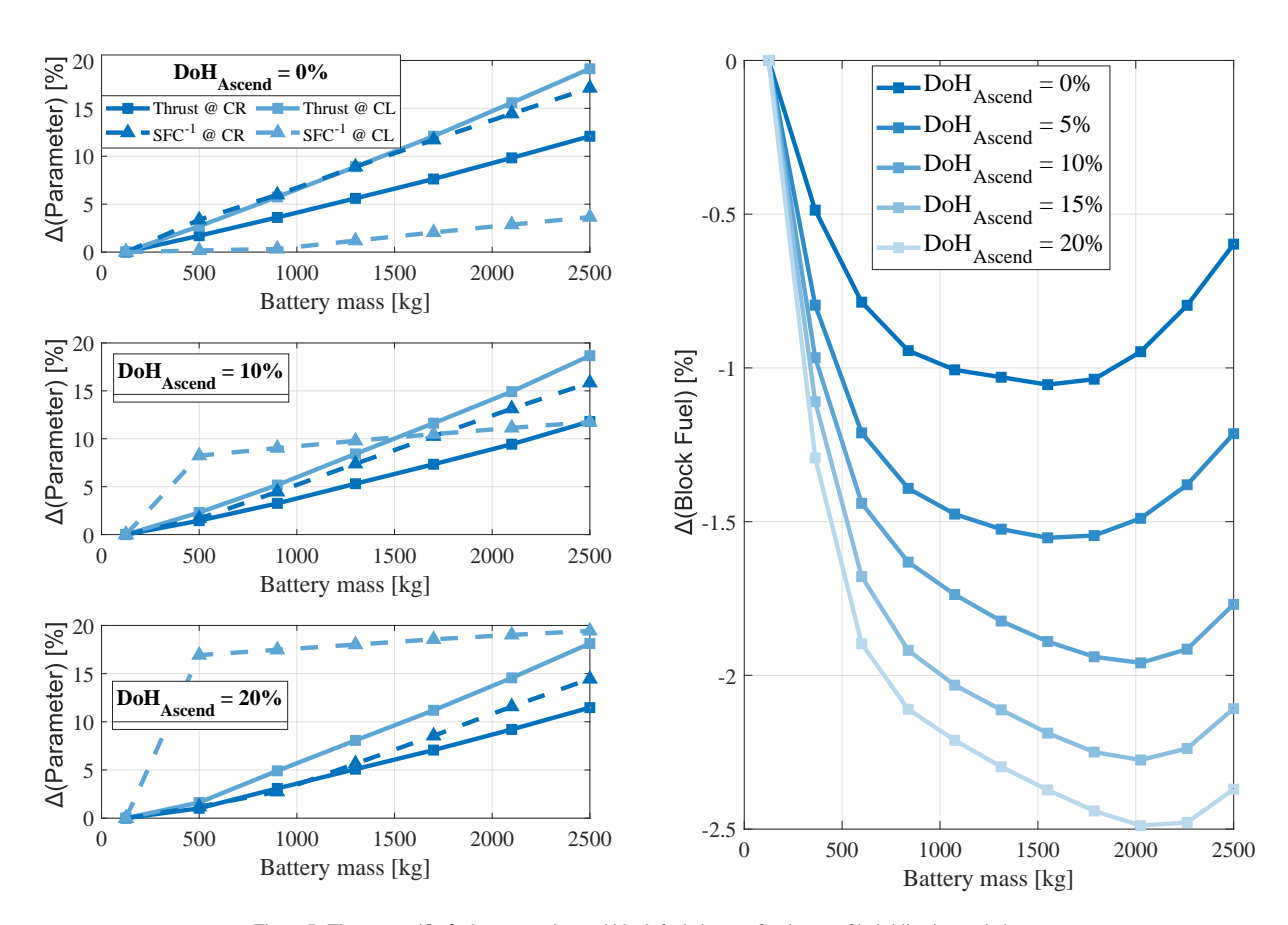


Figure 7: Thrust, specific fuel consumption and block fuel changes for degree of hybridization variations

3.2.2 Integrated Propulsion and Aircraft Design

The rapid increase of aircraft mass due to the electrical power system, generates a need to design both aircraft and propulsion system for prescribed take-off, climb and landing performance. The first two can be achieved by sole propulsion system design choices. However, landing performance and approach speed are also dictated by wind design. This simultaneous aircraft and propulsion system design is evaluated. Mission-level impacts of optimal FPT speed selection, descent one engine-off and distributed propulsion are also included (denoted as "Synergies" in following figures).

Figure 6 indicates that electrical power system introduction increases maximum take-off mass up to 25% in the examined design space. For the sole propulsion system design case of **Section 3.2.1**, wing area was kept constant at the value derived from the turboelectric configuration of $400 \ kg/m^2$. In **Section 3.2.2**, redesigned wings for landing and take-off TLARs increase in size by 25-50% in area, across the design space. This results in a further 5% increase of aircraft mass across the design space. Consequently, thrust requirement also raises by roughly the same amount. Keeping in mind the SFC improvements by electrification presented in **Section 3.2.1**, block fuel outcomes are shown in **Figure 8**.

Implementing the electrification scheme via sole propulsion system design, without considering top-level aircraft requirements, results in an up to 2.5% fuel benefit. This is pushed to 4% when the synergetic concepts are integrated, with the majority of additional advantages coming from turning off one turboshaft during descent. Distributed propulsion brings benefits through wing size reduction according to TLAR design conditions. Given that those are not active in this case, DP is not included as a synergy. The configuration with the integrated aircraft and propulsion system design, that matches all original top-level aircraft requirements, yields a 3-6% increase of block fuel across the design space, with no level of electrification being favorable when compared to the unconstrained turboelectric reference case. The synergetic concepts in the integrated design case, also include the impact of distributed propulsion, and improve fuel consumption by about 4% when accounted. The effect of the heavy electrical power system on the design wing and thrust loading is shown by the change of average trendlines for each examined case. When TLARs are matched, optimal battery mass is than 1000 kg, and more than doubles when TLARs are relaxed.

An investigation of different aspect ratios for the new series aircraft configurations revealed that optimal performance comes at a value of 12. However, the extra benefit amounts to less than 0.5% compared to the selected value of 11. Furthermore, to allow a point of commonality between the investigated and reference conventional and turboelectric cases, aspect ratio has been kept constant at 11. Conventionally, higher aspect ratios perform aerodynamically better, despite the added mass. However, in distributed propulsion concepts, high aspect ratios also inhibit the potential of having a greater fraction of the wing within the propeller jet airflow. Hence, the optimal performance aspect ratio value. Finally, while relaxing and not matching top-level aircraft requirements is bene-

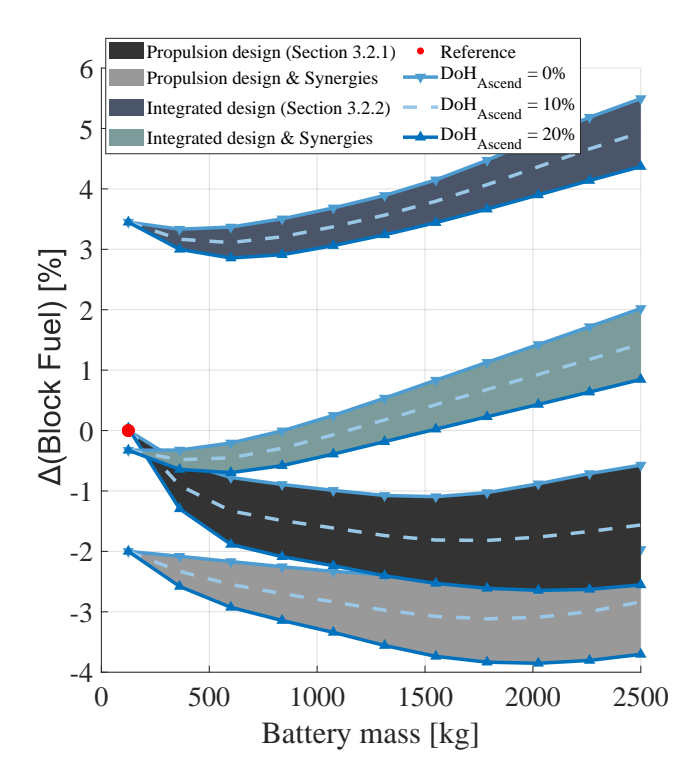


Figure 8: Block fuel variation for sole propulsion and integrated design approaches

ficial, wing loading ranges 400-500 kg/ m^2 , which pushes the structural limits at the higher end. In the redesigned wing case, it comes at 340 kg/ m^2 . For higher approach speeds, even smaller and more loaded wings (also closer to the 400 kg/ m^2 of the conventional EIS 2035 configuration) could be designed, yielding further performance benefits.

3.3 Sensitivity to Battery Technology

All prior investigations are for 0.6 kWh/kg cell specific energy. Actual battery energy density depends on technology advancements. Thus, the targets needed to facilitate competitive regional series hybrid electric aircraft are evaluated in **Figure 9**. Assumed cell specific energy is varied for 0.45-1.2 kWh/kg, for the median case of 10% ascend degree of hybridization. Battery mass varies and indicates cruise hybridization. Both design approaches are shown, including their respective synergies. Greater battery technologies result to more installed electrical energy, therefore the degrees of hybridization increase towards the top right corner, shown with the light gray isolines. Reference for normalizing outcomes is the unconstrained turboelectric concept.

Implementation of the hybridization scheme and propulsion design, without any top-level aircraft requirements being matched, yields up to 14% reduction of block fuel, accounting for synergies. Compared to the reference conventional aircraft, from which all the novel designs are derived, the reference unconstrained turboelectric leads to a 12% block fuel increase (**Table 1**). Hence, the relaxed TLAR series concepts with synergies, break even with the conventional EIS counterpart for assumed cell specific energy above 1.05 kWh/kg and 20% hybridization. The integrated propulsion and air-

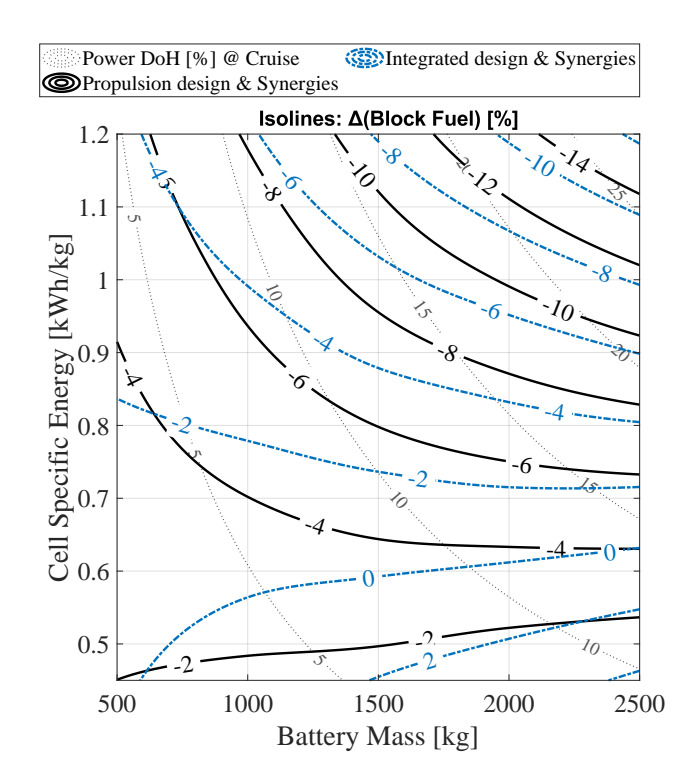


Figure 9: Change in block fuel and degree of hybridization at cruise for varying battery technology and mass

craft design approach, accounting for TLARs and synergies, consumes on average 2-4% more block fuel, compared to the unconstrained case. Hence, some TLAR compromise needs to be made, if a series hybrid electric concept is to be comparable with the same EIS conventional counterpart. Furthermore, in **Figure 9**, a cell specific energy threshold is observed, above which it is beneficial to electrify cruise further. This is roughly 0.6 kWh/kg and 0.7 kWh/kg for the unconstrained and integrated design approaches with synergies, respectively.

Environmental performance is investigated in **Figure 10** and shown only for the integrated design and synergies case. CO_2 trends follow block fuel closely. NO_x is also driven by combustor inlet conditions, which depend on thrust requirements and slightly shift the dominant trends imposed by fuel consumption. NO_x emissions are roughly 2% harder to bring down with electrification, and they also diminish with a reduced rate compared to CO_2 , as hybridization increases. This is observed in the top right corner, where the relative deviation between the two emissions expands to 4%.

3.4 Flight and operational conditions

Flight boundary conditions and business flight profiles are investigated in **Figure 11**. The "integrated design with synergies" case is evaluated, as it is the most realistic option. The turboelectric aircraft acts as the reference for relative outcomes. The median case of 10% design ascend hybridization and 1000 kg installed battery mass of 0.6 kW/kg is chosen as the baseline aircraft design for this evaluation. Further design details and top-level requirements are listed in **Table 1**.

Block specific range is defined as the distance covered per kilogram of fuel expended from take-off until landing, while

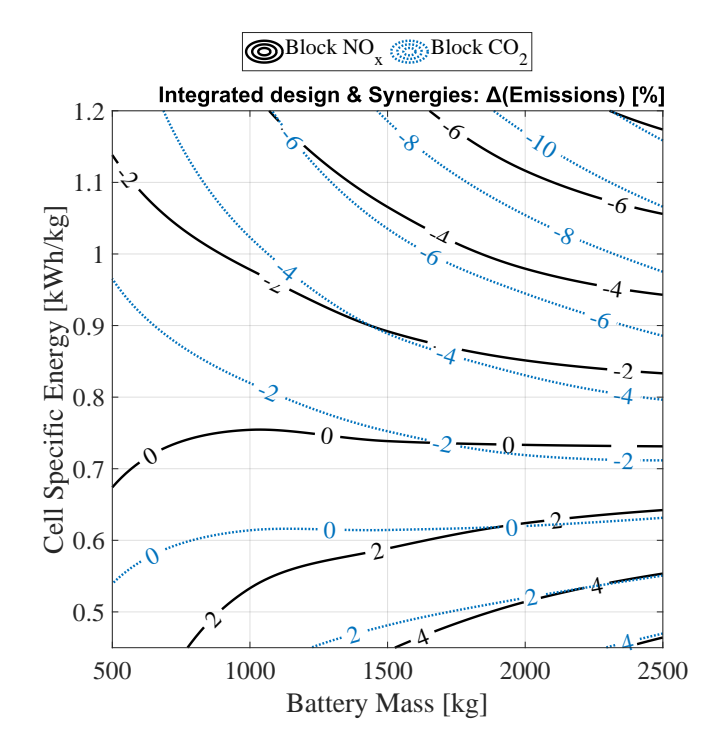


Figure 10: Environmental performance for varying battery technology and mass

main mission range includes climb to descent. Taxiing is omitted as it does not contribute towards the scheduled range. For increasing design and operation cruise altitude, aircraft specific range improves for all hybridization schemes and designs examined. This is attributed to the reduction of drag components due to ambient conditions, hence the increase of lift-over-drag ratio and reduction of required thrust. Flying at a higher altitude also slightly favors greater cruise degrees of hybridization, as is shown by the optimal design markers. Due to better aerodynamics at higher altitudes, heavier batteries are penalized less, hence more electrification benefits can be accrued. Design cruise Mach number is evaluated, revealing that block specific range improves for slower cruise operation. Aerodynamics are again more favorable at lower speeds for the turboprop aircraft. However, this dependency does not impact hybridization trends. It is noted that majority of these operational and flight trends are also applicable to a conventional aircraft case.

Finally, the operational (business) range options of a series hybrid electric aircraft with a design range of 1000 nmi are examined. For this design space, a fixed propulsion and aircraft design are evaluated, operating in different mission ranges, while the two previous cases of **Figure 11** referred to fromscratch designs for each data point of their design space. The aircraft is assumed to have a fixed mass of installed batteries, irrespectively of the business range selected, therefore, all installed electrical energy needs to be used until the 20% end-of-mission limit. For each examined business range different from the design one, the impact of changing the ascend phase is evaluated and found to have a near-zero effect. Since the propulsion system is fixed, either choosing to electrify more on ascend and less on cruise, or vice versa, intensifies the hybridization benefits of one segment at the nearly

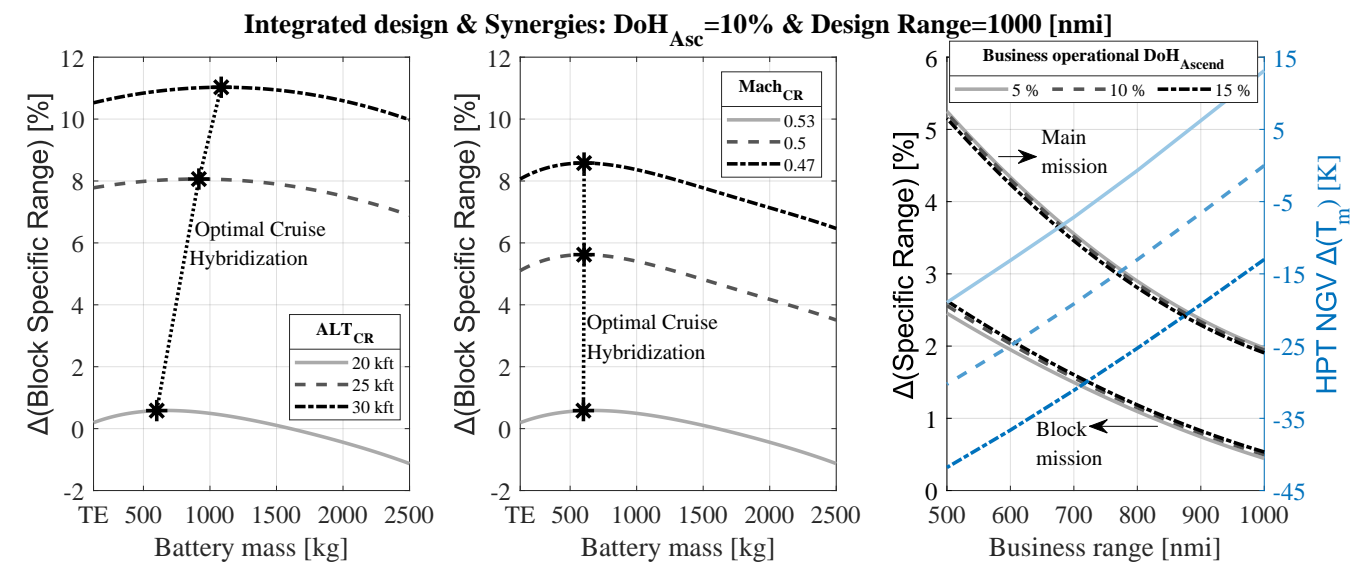


Figure 11: Specific aircraft performance under different operational scenarios

equal cost of the other's. Nevertheless, greater operational ascend hybridization is marginally beneficial for block specific aircraft range. Furthermore, it reduces the operational metal temperature of the high-pressure turbine nozzle guide vane by roughly 15 K, which can be beneficial for the engine's life expectancy, or allow for a hotter and more efficient cycle to be designed. Take-off and climb top-level requirements are matched also during business operation, hence, the lighter aircraft of shorter mission needs to operate at lower take-off and climb thrust ratings, thus, the reduction of engine temperatures in that direction as well. Operating the designed system at shorter missions, improves specific range, since more electrification can be scheduled, thus fuel consumption reduces further. Namely, at 1000 nmi range, cruise hybridization is about 5%, while it reaches 13% at 500 nmi. Main mission specific range is also shown to highlight that the benefit comes mostly from the cruise specific improvement. A conventional aircraft would not experience the parabolic benefit in specific range for reducing business range, that is related to the aforementioned increased cruise hybridization. Specific range would deteriorate given that the well-designed cruise segment mission fraction would reduce with business range.

4 Conclusions

An integrated methodology combining turboshaft, propeller, electrical and aircraft power system design is developed and deployed for the assessment of the series hybrid electric architecture. A 30-passenger regional aircraft with 1000 NMI design mission is investigated. Distributed propulsion with three propellers per wing provides benefits of 4% in drag reduction. Decoupling the propulsors and free power turbines offers potential for specific fuel consumption benefits. Proper speed selection can avoid performance and mass penalties in the order of 4% across different mission phases. However, those speeds already lie close to the reference single speed free power turbine design. Another 2% of fuel sav-

ings is unlocked by turning off one turboshaft engine during descent. Investigating optimal hybridization for the series concept, highlights that best results come from a combined ascend and cruise electrification. Cruise hybridization is favorable, up to he point where excessive battery mass triggers the aircraft weight and thrust snowball effect. Battery cell specific energy of 1-1.2 kWh/kg is the threshold for a series hybrid electric configuration to reach the emissions and fuel consumption savings of conventional Jet-A Entry-Into-Service 2035 aircraft, when both are compared to the Entry-Into-Service 2014 baseline. Shorter business range than the design improve specific aircraft range for the series hybrid electric configuration. Overall, it becomes apparent that some compromise in top-level aircraft requirements is necessary for the electrified aircraft to become one of the potential sustainable aviation solutions of the foreseeable future.

5 Acknowledgments

This work has been financed by the research project THEMIS, funded by the Knowledge Foundation (pr. no. 20200260).

References

- [1] D. Bermperis, M. D. Kavvalos, S. Vouros, and K. G. Kyprianidis. Mapping the potential of hybrid electric architectures for commuter aircraft. In *Proceedings of the ASME Turbo Expo*, Memphis, USA, June 2025.
- [2] M. Iwanizki, M. Arzberger, M. Plohr, D. Silberhorn, and T. Hecken. Conceptual design studies of short range aircraft configurations with hybrid electric propulsion. In *AIAA Aviation 2019 Forum*, Dallas, USA, 2019.
- [3] G. Cinar, Y. Cai, M. V. Bendarkar, A. I. Burrell, R. K. Denney, and D. N. Mavris. System analysis and design space exploration of regional aircraft with electrified powertrains. In *AIAA SCITECH 2022 Forum*, page 1994, San Diego, CA and Virtual, 2022.

- [4] C. P. Nasoulis, G. Protopapadakis, E. G. Ntouvelos, V. G. Gkoutzamanis, and A. I. Kalfas. Environmental and techno-economic evaluation for hybridelectric propulsion architectures. *The Aeronautical Journal*, 127(1317):1904–1926, 2023.
- [5] Tyler S. Dean, Gabrielle E. Wroblewski, and Phillip J. Ansell. Mission analysis and component-level sensitivity study of hybrid-electric general-aviation propulsion systems. *Journal of Aircraft*, 55(6):2454–2465, 2018.
- [6] J. Ludowicy, R. Rings, D. F. Finger, and C. Braun. Sizing studies of light aircraft with serial hybrid propulsion systems. Technical report, Deutsche Gesellschaft für Luft-und Raumfahrt-Lilienthal-Oberth eV, 2018.
- [7] Jonas Schroeter, Fabian Armbrüster, Reinhold Schaber, and Volker Gümmer. Optimization of a battery electric hybrid propulsion system for a short range aircraft. In *Turbo Expo: Power for Land, Sea, and Air*, volume 87929, page V001T01A037. ASME, 2024.
- [8] R. De Vries, M. Brown, and Roelof Vos. Preliminary sizing method for hybrid-electric distributed-propulsion aircraft. *Journal of Aircraft*, 56(6):2172–2188, 2019.
- [9] Yiyuan Ma, Chaofan Wang, Zhonghua Han, and Yue Wang. Mid-fidelity aero-propulsive coupling approach for distributed propulsion aircraft. *Aerospace Science* and Technology, 157:109859, 2025.
- [10] Borer N. K., Derlaga J. M., Deere K. A., Carter M. B., Viken S., Patterson M. D., Litherland B., and Stoll A. Comparison of aero-propulsive performance predictions for distributed propulsion configurations. In 55th AIAA Aerospace Sciences Meeting, page 0209, 2017.
- [11] Dennis Keller. Towards higher aerodynamic efficiency of propeller-driven aircraft with distributed propulsion. *CEAS Aeronautical Journal*, 12(4):777–791, 2021.
- [12] Konstantinos Kyprianidis. An approach to multidisciplinary aero engine conceptual design. In *Inter*national Symposium on Air Breathing Engines (ISABE 2017), Manchester, United Kingdom, 2017. Paper No. ISABE-2017-22661.
- [13] Konstantinos G. Kyprianidis. Future Aero Engine Designs: An Evolving Vision. IntechOpen, UK, 2011.
- [14] Kavvalos M. D., Bermperis D., Goinis G., Kaiser D., and Kyprianidis K. G. On the performance of commoncore turboprops. In *Proceedings of the ASME Turbo Expo*, Memphis, Tennessee, USA, June 2025.
- [15] D. Bermperis, M. D. Kavvalos, S. Vouros, and K. G. Kyprianidis. Advanced power management strategies for complex hybrid-electric aircraft. In *Proceedings of the ASME Turbo Expo*, volume 87929, page V001T01A039, London, UK, June 2024. American Society of Mechanical Engineers.

- [16] HECARRUS consortium. Wp2: Integrated systems level and powertrain architecture optimization. d2.3: Sizing, layout and performance of critical technologies. Deliverable D2.3, HECARRUS Project, 2022.
- [17] D. Bermperis, E. Ntouvelos, M. D. Kavvalos, S. Vouros, K. G. Kyprianidis, and A. I. Kalfas. Synergies and tradeoffs in hybrid propulsion systems through physics-based electrical component modeling. *Journal of Engineering for Gas Turbines and Power*, 146(1):011005, 2024.
- [18] M. Chen and G. A. Rincon-Mora. Accurate electrical battery model capable of predicting runtime and iv performance. *IEEE Transactions on Energy Conversion*, 21(2):504–511, 2006.
- [19] Lloyd R. Jenkinson, Paul Simpkin, Darren Rhodes, and Rolls Royce. *Civil Jet Aircraft Design*, volume 338. Arnold, London, 1999.
- [20] Jan Roskam. Airplane Design. DARcorporation, 1985.
- [21] E. Torenbeek. Synthesis of Subsonic Airplane Design: An Introduction to the Preliminary Design of Subsonic General Aviation and Transport Aircraft, with Emphasis on Layout, Aerodynamic Design, Propulsion and Performance. Springer Science & Business Media, 2013.
- [22] K. G. Kyprianidis and E. Dahlquist. On the trade-off between aviation nox and energy efficiency. *Applied Energy*, 185:1506–1516, 2017.
- [23] H. D. Yao, Z. Huang, L. Davidson, J. Niu, and Z. W. Chen. Blade-tip vortex noise mitigation traded-off against aerodynamic design for propellers of future electric aircraft. *Aerospace*, 9(12):825, 2022.
- [24] Z. Huang, H. Yao, A. Lundbladh, and L. Davidson. Low-noise propeller design for quiet electric aircraft. In AIAA Aviation 2020 Forum, page 2596. AIAA, 2020.
- [25] F. Salucci, C. E. Riboldi, L. Trainelli, A. L. Rolando, and L. Mariani. A noise estimation procedure for electric and hybrid-electric aircraft. In AIAA Scitech 2021 Forum, page 0258. AIAA, 2021.
- [26] D. Keller. Towards higher aerodynamic efficiency of propeller-driven aircraft with distributed propulsion. *CEAS Aeronautical Journal*, 12(4):777–791, 2021.
- [27] Michael D. Patterson. *Conceptual design of high-lift propeller systems for small electric aircraft*. Doctoral dissertation, Georgia Institute of Technology, 2016.